

COMPRESSION SET OF PU FOAM MATTRESSES WITH SELF-CLAMPING JOINTS AND SANDWICH STRUCTURE

MARTIN BOLDIŠ

SECONDARY VOCATIONAL SCHOOL OF WOODWORKING
TOPOLČANY, SLOVAK REPUBLIC

MIROSLAV GAŠPARÍK, MILAN GAFF, DANIEL RUMAN

CZECH UNIVERSITY OF LIFE SCIENCES, FACULTY OF FORESTRY AND WOOD SCIENCES
DEPARTMENT OF WOOD PROCESSING
PRAGUE, CZECH REPUBLIC

(RECEIVED FEBRUARY 2015)

ABSTRACT

This paper deals with research on the impact of composition on compression set of the PU foam mattresses. Three type of mattress composition, with sandwich structure and self-clamping joints, were used for research. The fourth type, which contained traditional glued joint, served as a reference. During static compression of mattresses, the properties of the individual layers have been recorded or calculated, such as Young's modulus, shear modulus and coefficient of shear friction, which were necessary for the SolidWorks simulation of the permanent deformation. The results, as well as simulations of mattress compositions, have proven that the compression set is strictly dependent on the loading time. The highest permanent deformation was recorded for mattress type A and the lowest ones for mattress type B, which had permanent deformation almost identical to that of the composition with glued joints. The last two mattress types had permanent deformation 35 % greater. It is clear from the results that the properties of self-clamping joints in upholstery can equal those of conventional glued joints. Using self-clamping joints is more advantageous in that they exclude the negative effects of glues as well as the gluing process itself.

KEYWORDS: Polyurethane foam; compression set; self-clamping joints; glued joint; mattresses.

INTRODUCTION

Together with spring mattresses, foam mattresses are currently among the most widely used mattresses. A high-quality foam mattress can provide good pressure support while copying body's shape and its weight. Foam mattresses are made of materials with various properties such

as standard polyurethane (PU), viscoelastic (memory or low-resilience) (Gama et al. 2015), cold (high-resilience), as well as latex foams.

Standard PU foams provide good flexibility, low weight, and a balanced stiffness-to-weight ratio. However, they may degrade over time and they deform more rapidly than, for example, viscoelastic foams. For this reason, they are used for common types of upholstered furniture having standard requirements. The current trend is to produce PU foams based on biomaterials (e.g., soy polyols) instead of crude oil (Faruk et al. 2014). Viscoelastic foams characteristically adjust to the pressure of the human body due to its temperature, thereby ensuring the necessary weight distribution. They are used in upholstered furniture designed for heavy loads or long use (in hospitals and retirement homes). Their disadvantage is the direct dependence on the surrounding temperature. Cold foams characteristically return rapidly to their original shape after load removal and have high elasticity, good breathability, and colder surfaces. Latex foams are the most suitable for such upholstered products as pillows, mattresses, and cushions (Ramasamy et al. 2013). They have good flexibility, softness, and shape retention and are also suitable for people with allergies or susceptible to asthma as they are hypoallergenic and resistant to dust. On the other hand, they are more dense, release liquids less readily, and degrade under UV radiation.

Polyurethane foams are traditionally and most commonly produced by reacting a di- or polyisocyanate with a polyol (Alzoubi et al. 2014). Both isocyanates and polyols used to produce PUs contain on average two or more functional groups per molecule. PU foams are materials widely used in various industries (civil engineering, automotive, packaging, and furniture) due to their low weight, high porosity, energy absorption, good thermal insulation, and formability (Tu et al. 2001, Marsavina et al. 2013b, Ma et al. 2013, Subramaniyan et al. 2013, Gama et al. 2015, Yan et al. 2015). In the furniture industry, they are used almost exclusively in upholstered furniture. PU foams comprise a broad key group of shaping and softening materials in both sandwich and zone structures for chair and bed furniture (Jin et al. 2007, Smardzewski and Matwiej 2015). In products with sandwich structures, PU foams can be used mainly in the central layers (Marsavina et al. 2013a, 2015, Espadas-Escalante and Avilés 2015, Şerban et al. 2016). Of the entire range of densities, only PU foams with densities 10 - 200 kg·m⁻³ are used in upholstery.

Among basic properties of PU foams is their compression set. Compression set, influenced by temperature and humidity, is a very important property and so most producers have defined specific tests and criteria for the suitability of individual foam types. In general, this property represents the material's ability to withstand irreversible deformations under a specific force. For example, two foam types that are almost identical can have very different compression sets as a result of this property's dependence on testing conditions (Sonnenschein et al. 2007). Foam's compression set depends on its material properties characterized by Young's modulus, the shear modulus, and Poisson's ratio. Standard PU foams are typical examples of isotropic materials that behave according to the classical theory of elasticity, i.e. a homogenous isotropic 3D object has Poisson's ratio ranging between -1 and 0.5 (Bezazi and Scarpa 2007, 2009).

Our goal is to expand knowledge on the impact of various PU foam sandwich composites on mattresses' compression sets. All the designed compositions with self-clamping joints were compared with glued mattresses. For the simulation of stresses the SolidWorks® package was used.

MATERIAL AND METHODS

Materials

Test samples were made by combining PU foams with various densities and properties according to four sandwich structure types (Fig. 1).

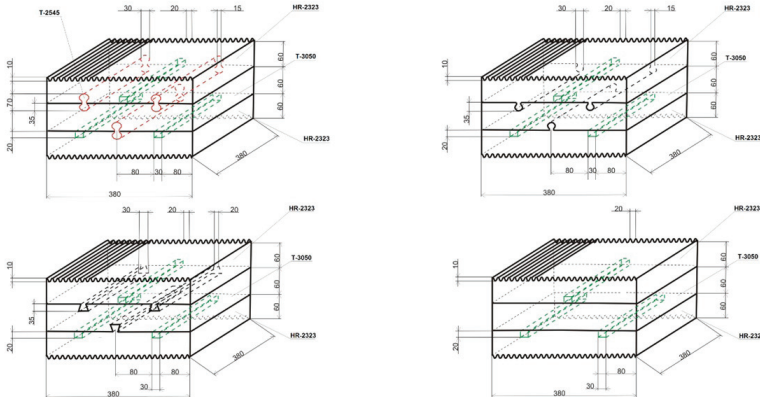
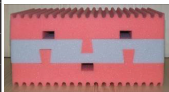
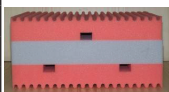


Fig. 1: Dimensions of individual samples of mattresses.

Three mattress composition types had self-clamping joints while the last type with a common joint served as a reference sample (Tab. 1). Mattress samples, with the dimensions of 180 x 380 x 380 mm, were prepared according to EN ISO 1923 (1995). A total of 5 samples of each mattress type were used for the experiment.

Tab. 1: Material composition for individual mattress types.

Mattress type	Mattress structure	Mattress composition	Joint type	Sandwich composition
A	sandwich	YUMA 7573 three-layer covering fabric	self-clamping joint with tongue-in-groove (double drop)	
		HR-2323 PUR fitment		
		T-2545 PUR self-clamping joint		
		T-3050 PUR fitment		
		T-2545 PUR self-clamping joint		
		HR-2323 PUR fitment		
YUMA 7573 three-layer covering fabric				
B	sandwich	YUMA 7573 three-layer covering fabric	self-clamping joint with tongue and groove (single drop)	
		HR-2323 PUR fitment		
		T-3050 PUR fitment		
		HR-2323 PUR fitment		
		YUMA 7573 three-layer covering fabric		

C	sandwich	YUMA 7573 three-layer covering fabric	self-clamping joint with tongue and groove (dovetail)	
		HR-2323 PUR fitment		
		T-3050 PUR fitment		
		HR-2323 PUR fitment		
		YUMA 7573 three-layer covering fabric		
D	sandwich	YUMA 7573 three-layer covering fabric	glued joint	
		HR-2323 PUR fitment		
		T-3050 PUR fitment		
		HR-2323 PUR fitment		
		YUMA 7573 three-layer covering fabric		

Tab. 2: Technical parameters of PUR foam types (Boldiš 2009).

Type of tested PUR foam		Color	Apparent density	CLD - hardness (40 %)	Tensile strength	Compression set	SAG factor
			EN ISO 845 (2006)	ISO 3386-1 (1986)	ISO 1798 (2008)	EN 1856 (2001)	EN ISO 2439 (2008)
Standard marking	Alternative marking		(kg.m ⁻³)	(kPa)	(kPa)	(%)	min. 2.5
			range	range	min. 90	(72h)	
T-2545	T-25 180 (T-25H)	light grey	22.5 – 25.5	3.83 – 5.18	160	3 max. 8	–
T-3050	T-30 200	light blue	27.5 – 30.5	4.25 – 5.75	170	2.5 max. 7	–
HR-2323	HR-23 090	pink	20.5 – 23.5	1.96 – 2.65	110	6.0 max 7	2.8

Methods

Compression set

At the beginning, samples were conditioned for 16 hours at the temperature of 23 ± 0.5 °C and relative humidity of 50 ± 5 %. After conditioning period, the sample thicknesses were measured according to EN ISO 1923 (1995) and EN 1334 (2001). The final value of the mattress's thickness was the average of the four measurements.

The sample was inserted between the two flat plates (Fig. 2) of compression device with dimensions larger than the samples. Subsequently, the samples were compressed to 50 ± 4 % of their original thickness under the conditioning conditions. After the 2, 4, 24, 48, and 72 hours, the loading was interrupted and the samples were quickly measured again. Then, the samples were compressed again. After the 72 ± 0.2 hours loading, the apparatus was removed and the samples recovered for 30 ± 5 minutes on a wooden surface under the same conditions. The last thickness measurement was done after 10 days of the recovery. The compression set for each time period was calculated. Whole experiment for determining the compression set was carried out according to EN ISO 1856 (2001) using a Method C.

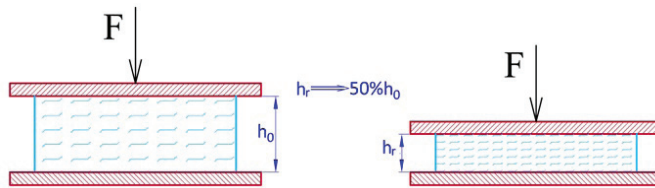


Fig. 2: Principle of compression set testing.

Measurements

The values for maximum loading force were downloaded from the data logger onto a computer and the Young's modulus in compression and shear modulus was calculated. Poisson's ratio was set to 0.3, which is applicable to most materials including standard polyurethane foam (Greaves et al. 2011).

Simulation

For simulation of real mattress behavior, it was necessary to know both the physical and mechanical properties of the individual layers in the SolidWorks®, 2010 application. The isotropic linear model required Young's moduli in compression, shear moduli, Poisson's ratios, as well as shear friction coefficients of individual layers (Tabs. 1 - 4).

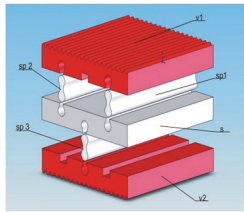


Fig. 3: Mattress sample, type A (v1, v2 – upper/lower layers; s – middle layer; sp1, sp2, sp3 – joints).

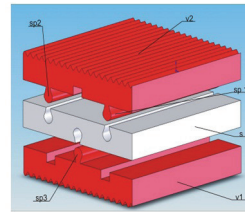


Fig. 4: Mattress sample, type B (v1, v2 – upper/lower layers; s – middle layer; sp1, sp2, sp3 – joints).

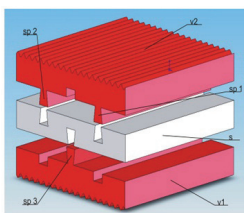


Fig. 5: Mattress sample, type C (v1, v2 – upper/lower layers; s – middle layer; sp1, sp2, sp3 – joints).

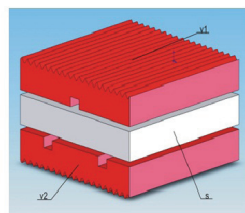


Fig. 6: Mattress sample, type D (v1, v2 – upper/lower layers; s – middle layer).

The simulation was done for three types of self-clamping joints as well as glued joint.

Mechanical characteristics of all layers for four mattress types are shown in (Tabs. 3 - 4). For the simulation only the data for maximum loading of 72 h were used.

Tab. 3: Mechanical properties of all mattress types after compression set test.

Mattress type	Layers	Poisson's ratio	Loading yield force F _y (N)	Young's modulus in compression E (MPa)			Shear modulus G (MPa)		
				2 h	72 h	240 h	2 h	72 h	240 h
A	v ₁	0.3	-	0.250	0.077	0.695	0.096	0.030	0.267
	v ₂	0.3	-	0.210	0.058	0.359	0.081	0.022	0.138
	s	0.3	-	0.071	0.029	0.061	0.027	0.011	0.023
	sp ₁	0.3	-	1.045	0.512	1.395	0.402	0.197	0.537
	sp ₂	0.3	-	1.679	0.513	1.679	0.646	0.197	0.646
	sp ₃	0.3	-	1.197	0.428	1.395	0.460	0.165	0.537
	Mattress as a whole	0.3	1753	0.713	0.194	0.784	0.274	0.075	0.302
B	v ₂ + sp ₁ + sp ₂	0.3	-	0.741	0.305	1.558	0.285	0.117	0.599
	v ₁ + sp ₃	0.3	-	0.764	0.321	1.733	0.294	0.123	0.667
	s	0.3	-	1.936	0.442	5.807	0.745	0.170	2.233
	Mattress as a whole	0.3	2143	0.847	0.388	2.265	0.326	0.149	0.871
C	v ₂ + sp ₁ + sp ₂	0.3	-	0.904	0.196	0.497	0.348	0.075	0.191
	v ₁ + sp ₃	0.3	-	0.530	0.176	0.854	0.204	0.068	0.328
	s	0.3	-	5.028	0.450	1.328	1.934	0,173	0.511
	Mattress as a whole	0.3	2758	0.670	0.225	0.617	0.258	0.087	0.237
D	v ₁	0.3	-	0.190	0.092	0.348	0.073	0.035	0.134
	v ₂	0.3	-	0.202	0.098	0.304	0.078	0.038	0.117
	s	0.3	-	0.734	0.266	0.729	0.282	0.102	0.280
	Mattress as a whole	0.3	1786	0.578	0.286	0.678	0.222	0.110	0.261

Tab. 4: Coefficient of shear friction between individual mattress layers.

Combination of layers	LFB – v1	LFB – v2	v2 – sp	v1 – s	sp – s	v1 – sp
Coefficient of shear friction k _s	1.106	1.2799	1.2349	2.4751	1.3764	1.428

*Note: LFB – laminated fiberboard, v₁, v₂ – upper/lower layers, s – middle layers, sp – joints.

Simulation procedures for compression set

The obtained data were analyzed and the simulation results were compared with real ones according to the following steps.

1. Drawing of 3-D models for designed types of foam mattresses using the SolidWorks application.
2. Transformation of 3-D models to COSMOS Works sub-application and input of boundary conditions for designed foam mattresses based on both identified factors and material properties of the used foam materials (Tabs. 1 to 4).
3. Creation of finite elements network in COSMOS Works sub-application. The assembly network consists of volume elements. In the structural assemblies, each node has three degrees of freedom within the volume element, representing the shifts in three orthogonal

directions. For the problem formulation, the software uses the directions X, Y, and Z of the global Cartesian system of coordinates. For the simulation purposes, a network consisting of linear volume tetrahedral elements has been used.

4. The simulation of permanent compression deformations (compression set) in the linear zone of the isotropic models by COSMOS Works sub-application.
5. Results evaluation.
6. Comparison of experimental results with simulations (Fig. 14).

Evaluation and calculation

The compression set (permanent deformation in compression) was calculated according EN ISO 1856 (2001) and Eq. 1:

$$c.s. = \frac{h_0 - h_r}{h_0} \times 100 \quad (1)$$

where: *c.s.* - compression set (%),
 h_0 - original height (thickness) of upholstery samples before testing (mm),
 h_r - height (thickness) of upholstery sample after recovery (mm).

The influence of mattress type and time of recovery on compression set was statistically evaluated using ANOVA, mainly by Fisher's F-test, in STATISTICA 10 software (Statsoft Inc.; USA).

The Young's modulus in compression was calculated according to Eq. 2:

$$E = \frac{F_y \cdot h_0}{S \cdot \Delta h} \quad (2)$$

where: E - Young's modulus in compression (MPa),
 F_y - loading force at yield point (N),
 S - actual cross-sectional area through which the force is applied (mm²),
 h_0 - original height (thickness) of the material,
 Δh - amount by which the height (thickness) of the material changes (mm).

Shear modulus was calculated according to Eq. 3:

$$G = \frac{E}{2(1 + \nu)} \quad (3)$$

where: G - shear modulus (MPa),
 E - Young's modulus in compression (MPa),
 ν - Poisson's ratio (-).

RESULTS AND DISCUSSION

A two-factor analysis was used to evaluate how the actual tested permanent deformation of various mattress types varied under pressure at various loading/recovery time. All factors are statistically significant (Figs. 7–8 and Tab. 5).

Tab. 5: Influence of factors on compression set.

Monitored factor	Sum of squares	Degree of freedom	Variance	Fisher's F-test	Significance Level P
Intercept	18422.4067	1	18422.4067	6802.1012	0.0000
Mattress type	1484.7588	3	494.9196	182.7391	0.0000
Loading/recovery time	2659.6595	5	531.9319	196.4051	0.0000
Mattress type * Loading/recovery time	875.3073	15	58.3538	21.5460	0.0000
Error	1495.0040	552	2.7083		

*Note: Statistical significance was evaluated at the 95 % confidence interval.

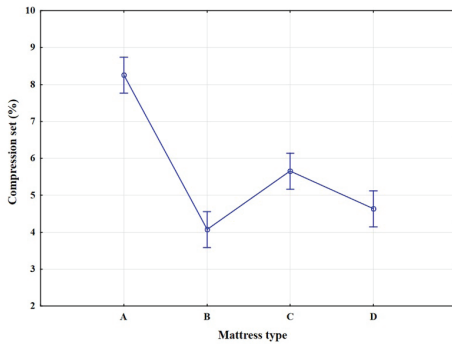


Fig. 7: Influence of mattress type on compression set.

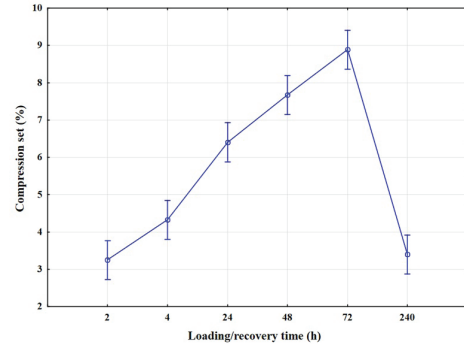


Fig. 8: Influence of loading/recovery time on compression set.

Fig. 9 depicts permanent deformation change with loading/recovery time and for all tested mattress types. After 2, 4, and 24 hours of loading the tested mattress samples with double drop (tongue-in-groove) self-clamping joints significantly differed from the other tested mattress samples. After 48 hours of loading, the tested mattress sample types with single drop and dovetail (tongue and groove) self-clamping joints also differed significantly from the mattress samples with double drop self-clamping joints. After 72 hours of loading, the significant differences in permanent deformation under pressure in the aforementioned mattress types widened. After 240 hours of the recovery, there was only significant difference between samples with dovetail self-clamping joints and the other tested samples. Throughout loading and recovery time, tested samples with single drop self-clamping joints did not differ significantly in permanent deformation from referenced glued samples. Samples with dovetail self-clamping joints did not conform to the reference sample mainly due to the large difference in permanent deformation after the load was removed.

The Figs. 10 to 13 show the course of deformations of sandwich structures during compression to 50 % of their thicknesses. The zones with the deformation highest values are marked with red color. The direction of compression deformations can be seen. The zone of highest deformations is located mainly in the area of contact between the compression plate and the sandwich top layer. With the acting force increase, the deformation of samples with self-clamping joints is apparent mainly in the area of deaeration hole as well as notched top layer. Both top and bottom layers are elongating and the middle layer remains almost unchanged. In the case

of glued sample D, almost uniform deformation occurs. It is concentrated in the sandwich top layer; whereas both top and bottom layers are extending slightly into the sides.

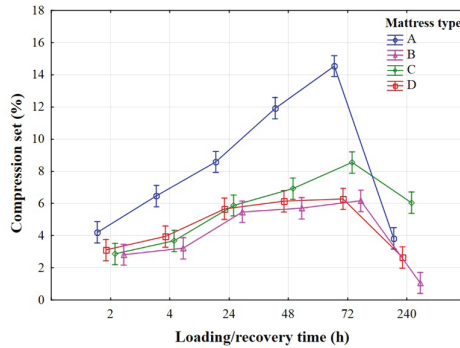


Fig. 9: Influence of mattress type and loading/recovery time on compression set.

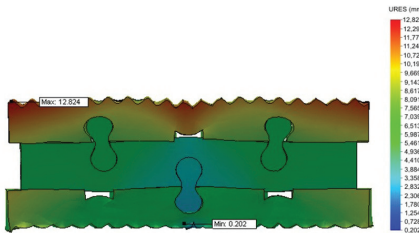


Fig. 10: Course of permanent deformation for composition A after 72 h loading.

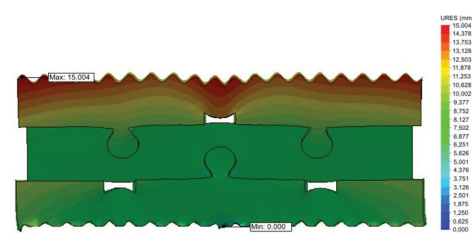


Fig. 11: Course of permanent deformation for composition B after 72 h loading.

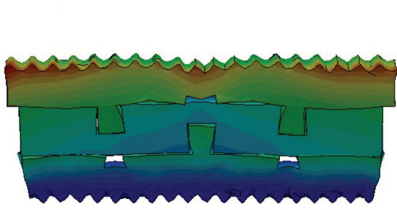


Fig. 12: Course of permanent deformation for composition C after 72 h loading.

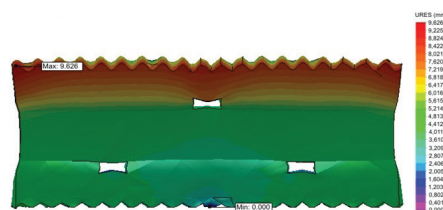


Fig. 13: Course of permanent deformation for composition D after 72 h loading.

Mattress types A, B and C had minimum simulated deformations in the areas of self-clamping joints; however, for the overall sandwich structures, these deformations were greater than for sample D.

Comparison of simulation with real deformation

Subsequently, the permanent compression deformation from the analysis was compared with real values of compression set. This comparison verified that the samples deformation was similar to that of real load obtained during testing (Fig. 14).

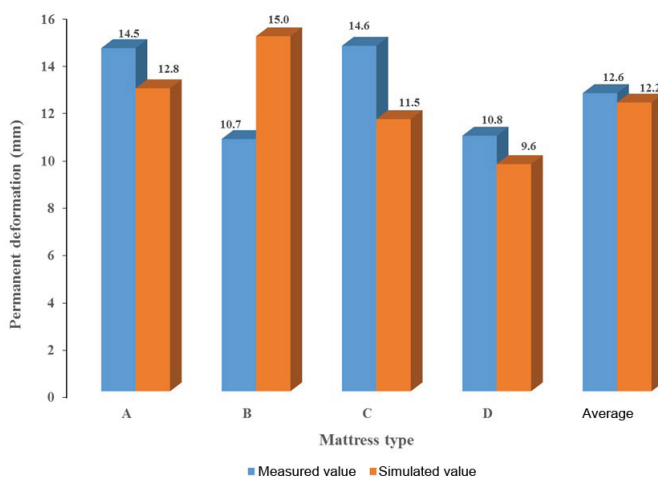


Fig. 14: Comparison of measured and simulated values of permanent deformation for the individual mattress types.

The simulated deformations for all sample types are apparently lower than the real measured values; however, they copy the real deformation courses. Only sample B had higher simulated values than those measured in reality. Therefore, we can conclude that the samples with glued joints achieved the lowest, both real and simulated values, of the permanent compression deformation. It means that the longest durability among the tested mattress types was proved. However, sample B achieved similar measured values as sample D.

CONCLUSIONS

The permanent deformation of both self-clamping joints as well as glued joint can be considered as the most important result. The following conclusion can be drawn: the foam mattresses with sandwich structure and glued joint are recommendable because of their durability. Glued joint shows the lowest deformations, so they are the most suitable among the compared joints. Mattresses with self-clamping joints achieve higher compression sets, although the difference to the compositions with glued joints is not very marked. Therefore, the compositions with self-clamping joints can be recommended as an alternative to the glued joints (also taking into account ecological aspects). Another contribution of the study is the fact that, the given material characteristics can be used in construction objective and precise models.

ACKNOWLEDGMENTS

The authors are grateful for the support of the University-wide Internal Grant Agency (CIGA) of the Faculty of Forestry and Wood Science, Czech University of Life Sciences, project 4308-2016. The authors would like to thank the Technical University in Zvolen, Slovakia for providing the testing laboratory and equipment.

REFERENCES

1. Alzoubi, M.F, Al-Hallaj, S., Abu-Ayyad, M., 2014: Modeling of compression curves of flexible polyurethane foam with variable density, chemical formulations and strain rates. *Journal of Solid Mechanics* 6(1): 82-97.
2. Bezazi, A., Scarpa, F., 2007: Mechanical behaviour of conventional and negative Poisson's ratio thermoplastic polyurethane foams under compressive cyclic loading. *International Journal of Fatigue* 29(5): 922-930, DOI: 10.1016/j.ijfatigue.2006.07.015.
3. Bezazi, A., Scarpa, F., 2009: Tensile fatigue of conventional and negative Poisson's ratio open cell PU foams. *International Journal of Fatigue* 31(3): 488-494, DOI: 10.1016/j.ijfatigue.2008.05.005.
4. Boldiš, M., 2009: The joints of polyurethane foams in upholstery for bed furniture. (Spoje polyuretánových penových materiálov v čalúnení lôžkového nábytku). PhD. Thesis, Technical University in Zvolen, Slovakia, 148 pp (in Slovak).
5. EN 1334, 1996: Domestic furniture - Bed and mattresses - Methods of measurement and recommended tolerances.
6. EN 1725, 1998: Domestic furniture - Bed and mattresses - Safety requirements and test methods,.
7. EN ISO 1798, 2008: Flexible cellular polymeric materials - Determination of tensile strength and elongation at break.
8. EN ISO 1856, 2001: Flexible cellular polymeric materials - Determination of compression set.
9. EN ISO 1923, 1995: Cellular plastics and rubbers - Determination of linear dimensions.
10. EN ISO 2439, 2008: Flexible cellular polymeric materials - Determination of hardness (indentation technique).
11. Espadas-Escalante, J.J., Avilés, F., 2015: Anisotropic compressive properties of multiwall carbon nanotube/polyurethane foams. *Mechanics of Materials* 91(1): 167-176, DOI: 10.1016/j.mechmat.2015.07.006.
12. Faruk, O., Sain, M., Farnood, R., Pan, Y., Yiao, H., 2014: Development of lignin and nanocellulose enhanced bio PU foams for automotive parts. *Journal of Polymers and the Environment* 22(3): 279-288, DOI: 10.1007/s10924-013-0631-x.
13. Gama, N.V., Soares, B., Freire, C.S.R., Silva, R., Neto, C.P., Barros-Timmons, A., Ferreira, A., 2015: Bio-based polyurethane foams toward applications beyond thermal insulation. *Materials & Design* 76: 77-85, DOI: 10.1016/j.matdes.2015.03.032.
14. Greaves, G.N., Greer, A.L., Lakes, R.S., Rouxel, T., 2011: Poisson's ratio and modern materials. *Nature Materials* 10(11): 823-837, DOI: 10.1038/nmat3134.
15. ISO 845, 2006: Cellular plastics and rubbers - Determination of apparent density.
16. ISO 3386-1, 1986: Polymeric materials, cellular flexible - Determination of stress-strain characteristics in compression -- Part 1: Low-density materials.
17. Jin, H., Lu, W.Y., Scheffel, S., Hinnerichs, T.D., Neilsen, M.K., 2007: Full-field characterization of mechanical behavior of polyurethane foams. *International Journal of Solids and Structures* 44(21): 6930-6944, DOI:10.1016/j.ijsolstr.2007.03.018.
18. Ma, Y., Su, X., Pyrz, R., Rauhe, J.Ch., 2013: A novel theory of effective mechanical properties of closed-cell foam materials. *Acta Mechanica Solida Sinica* 26(6): 559-569, DOI: 10.1016/S0894-9166(14)60001-X.

19. Marsavina, L., Constantinescu, D.M., Linul, E., Voiconi, T., Apostol, D.A., Sadowski, T., 2013a: Damage identification and influence on mechanical properties of closed cell rigid foams. In: Proceedings of the 13th International Conference on Fracture, June 16-21, Beijing, China.
20. Marsavina, L., Linul, E., Voiconi, T., Sadowski, T., 2013b: A comparison between dynamic and static fracture toughness of polyurethane foams. *Polymer Testing* 32(4): 673-680, DOI: 10.1016/j.polymertesting.2013.03.013.
21. Marsavina, L., Constantinescu, D.M., Linul, E., Apostol, D.A., Voiconi, T., Sadowski, T., 2015: Refinements on fracture toughness of PUR foams. *Engineering Fracture Mechanics* 129 (Macrofracture analysis and testing — 19th European Conference on Fracture (ECF19) selected papers). Pp 54-66, DOI: 10.1016/j.engfracmech.2013.12.006.
22. Ramasamy, S., Ismail, H., Munusamy, Y., 2013: Effect of rice husk powder on compression behavior and thermal stability of natural rubber latex foam. *BioResources* 8(3): 4258-4269, DOI: 10.15376/biores.8.3.4258-4269.
23. Şerban, D.A., Weissenborn, O., Geller, S., Marşavina, L., Gude, M., 2016: Evaluation of the mechanical and morphological properties of long fibre reinforced polyurethane rigid foams. *Polymer Testing* 49: 121-127, DOI: 10.1016/j.polymertesting.2015.11.007.
24. Smardzewski, J., Matwiej, Ł., 2015: Effect of aging of polyurethane foams in the context of furniture design. *Drvna Industrija* 64(3): 201-209, DOI: 10.5552/drind.2013.1241.
25. SolidWorks 2010: Version 4400. Dassault Systèmes SE, Vélizy-Villacoublay, France.
26. Sonnenschein, M.F., Prange, R., Schrock, A.K., 2007: Mechanism for compression set of TDI polyurethane foams. *Polymer* 48(2): 616-623, DOI: 10.1016/j.polymer.2006.11.021.
27. Subramaniyan, S.K., Mahzan, S., Ghazali, M.I., Ismon, M., Zaidi, A.M.A., 2013: Mechanical behavior of polyurethane composite foams from kenaf fiber and recycled tire rubber particles. *Applied Mechanics and Materials* 315: 861-866, DOI: 10.4028/www.scientific.net/AMM.3.31.861.
28. Tu, Z.H., Shim, V.P.W., Lim, C.T., 2001: Plastic deformation modes in rigid polyurethane foam under static loading. *International Journal of Solids and Structures* 38(50-51): 9267-9279, DOI: 10.1016/S0020-7683(01)00213-X.
29. Yan, R., Wang, R., Lou, Ch.-W., Mahmoudabadi, M.Z., 2015: Quasi-static and dynamic mechanical responses of hybrid laminated composites based on high-density flexible polyurethane foam. *Composites Part B: Engineering* 83: 253-263, DOI: 10.1016/j.compositesb.2015.08.037.

MARTIN BOLDIŠ
SECONDARY VOCATIONAL SCHOOL OF WOODWORKING
PILSKÁ 12
SK-955 01 TOPOLČANY
SLOVAKIA

*MIROSLAV GAŠPARÍK, MILAN GAFF, DANIEL RUMAN
CZECH UNIVERSITY OF LIFE SCIENCES
FACULTY OF FORESTRY AND WOOD SCIENCES
DEPARTMENT OF WOOD PROCESSING
KAMÝČKÁ 1176
CZ-165 21 PRAGUE 6 - SUCHDOL
CZECH REPUBLIC
PHONE: +420 22438 3828
Corresponding author: gathiss@gmail.com

